

Dark Energy as an Inverse Problem

Cristina Espa  -Bonet*

Department of Astronomy, University of Barcelona

and CER for Astrophysics, Particle Physics and Cosmology, Mart   i Franqu  s 1, Barcelona 08028, Spain

Pilar Ruiz-Lapuente†

Departament of Astronomy, University of Barcelona

and CER for Astrophysics, Particle Physics and Cosmology,

Mart   i Franqu  s 1, Barcelona 08028, Spain and

Max-Planck-Institut f  r Astrophysik, Karl Schwarzschild Stra  e 1, 85740 Garching, Germany

(Dated: December 2, 2024)

A model-independent approach to dark energy is here developed by considering the determination of its equation of state as an inverse problem. The reconstruction of $w(z)$ as a non-parametric function using the current SNe Ia data is explored. It is investigated as well how results would improve when considering other samples of cosmic distance indicators at higher redshift. This approach reveals the lack of information in the present samples to conclude on the behavior of $w(z)$ at $z > 0.6$. At low level of significance a preference is found for $w_0 < -1$ and $w'(z) > 0$ at $z \sim 0.2\text{--}0.3$. The solution of $w(z)$ along redshift never departs more than 1.95σ from the cosmological constant $w(z) = -1$, and this only occurs when using various cosmic distance indicators. The determination of $w(z)$ as a function is readdressed considering samples of large number of SNe Ia as those to be provided by SNAP. It is found an improvement in the resolution of $w(z)$ when using those synthetic samples, which is favored by adding data at very high z . Though the set of degenerate solutions compatible with the data can be retrieved through this method, these degeneracies in the solution will difficult the physical interpretation of the results. Through this approach, we have explored as well the gain in information in $w(z)$ and the quality of the inversion achieved using different data sets of cosmic distance indicators.

I. INTRODUCTION

The acceleration of the rate of expansion of the Universe, first discovered through supernovae [1, 2] is being confirmed by new cosmological tests. The cosmic microwave background measurements by the Wilkinson Microwave Anisotropic Probe (WMAP) [3] and results from the large scale distribution of galaxies [4] and galaxy clusters [5] confirm that our universe is dominated by negative pressure. The understanding of the accelerated expansion of the cosmos might result in a change of the framework in which gravity is to be described or in the identification of unknown components of the cosmos. All this seems most fundamental to physics and cosmology, thus large samples of cosmological data and various procedures to analyse them are being examined.

In a descriptive way, the component or new physics responsible for the acceleration of the expansion, the so called “dark energy”, can be incorporated in the right-hand side of the Friedmann–Robertson–Walker (FRW) equations and be simply addressed as an additional term for whom we intend to determine the barotropic index: $w(z) = p(z)/\rho(z)$.

The reconstruction of $w(z)$ from a given sample of data has been attempted proposing fitting functions or expansion series of $w(z)$ along z in ways to accomodate a wide

range of dark energy candidates [6–15]. There has been some debate on the effect that choosing particular models for those functions or truncating the expansion series in z might have in deriving possible evolution [13–16].

Here, we have developed an approach to obtain $w(z)$ without imposing any constraints on the form of the function. This is addressed through a generalized nonlinear inverse approach. This method allows to examine the resolution of the equation of state $w(z)$ at various redshifts and through various samples. One can quantify the improvement in information provided by an increased number of data or the addition of various data sources. The inverse approach formulated by Backus and Gilbert(1970)[17] has been widely used in geophysics and solar structure physics. In this approach, the mere fact that the continuous functional has to be derived from a discrete number of data implies a non-uniqueness of the answer. It has also been shown that, even if the data were dense and with no uncertainty, there would be more than one solution to many specific inverse problems such as the determination of the density structure of the earth from the data on the local gravitational field at its surface, and others. This lack of uniqueness comes from the way in which the different equations reflect in the observables used. The problem of the determination of dark energy faces such degeneracy. In the luminosity distance along z from supernovae and other cosmic distance indicators, $w(z)$ enters in an integral form, which limits the possibility to access to $w(z)$.

In earlier examinations of the degeneracy in $w(z)$ obtained through cosmic distance indicators a range of so-

*cespana@am.ub.es

†pilar@am.ub.es

lutions giving the same luminosity distance along z were pointed out [18, 19]. As more data would constrain $w(z)$ at various redshifts, not only using the distance luminosity, but other indicators as well, the reconstruction should become more successful.

To compare with a significant body of work which analyses the data using the expansion to first order $w(z) = w_0 + w_a z/(1+z)$, we will also formulate this approach for the case of determination of discrete parameters. This allows to quantify the increase of information among SNe Ia samples and samples of other distance indicators. We examine from current data the possibility of determining at present the values of $w(z)$ and its first derivative and compare with previous results [15, 20]. Finally, we will apply this reconstruction to find the data distribution which achieves a better quality in the inversion.

II. INVERSE PROBLEM

The inverse problem provides a powerful way to determine the values of functional forms from a set of observables. This approach is useful when the information along a certain coordinate, in our case information on $w(z)$, emerges in observables coupled with information at all other z . We have a surface picture of $w(z)$ in the luminosity distance at a given z , as the p-mode waves in the Sun surface have on its internal structure. Dark energy is here addressed using the non-linear non-parametric inversion. Most frequently, when the parameters to be determined are a set of discrete unknowns, the method used is a least squares. But the continuous case, where functional forms are to be determined, requires a general inverse problem formulation. The inverse approach version used here is a Bayesian approach to this generalization [21].

We consider a flat universe with only two dominant constituents (at present): cold matter and dark energy. Therefore we characterize the cosmological model by the density of matter, Ω_M , and by the index $w(z)$ of the dark energy equation of state,

$$w(z) = \frac{p(z)}{\rho(z)} \quad (1)$$

Our vector of unknowns M has then a discrete and a continuous component,

$$M = \begin{pmatrix} \Omega_M \\ w(z) \end{pmatrix} \quad (2)$$

Our observational data are mainly SNe Ia magnitudes. We have a finite set of N magnitudes, m^i , and consider the following theoretical equation, the magnitude-redshift relation in a flat universe relating the unknowns to the observational data:

$$m^{th}(z, \Omega_M, w(z)) = \mathcal{M} + 5 \log[D_L(z, \Omega_M, w(z))], \quad (3)$$

where

$$\mathcal{M} \equiv M - 5 \log H_0 + 25 \quad (4)$$

and D_L is the Hubble-free luminosity distance

$$D_L(z, \Omega_M, w(z)) = c(1+z) \int_0^z \frac{dz'}{\sqrt{\Omega_M(1+z')^3 + \Omega_X(z')}} \quad (5)$$

$$\Omega_X(z) = \Omega_X \exp \left(3 \int_0^z dz' \frac{1+w(z')}{1+z'} \right). \quad (6)$$

In order to combine the results with other data we substitute the original SNe magnitudes by the dimensionless distance coordinate y :

$$y_i \equiv \frac{\exp_{10}((m_i - \mathcal{M})/5)}{c(1+z_i)} = \int_0^{z_i} \frac{dz'}{\sqrt{\Omega_M(1+z')^3 + \Omega_X(z')}}, \quad (7)$$

$$\sigma_{y_i} = \frac{\ln 10}{5} y_i (\sigma_{m_i} + \sigma_{\mathcal{M}}). \quad (8)$$

With this definition we deal directly with a function $y(\Omega_M, w(z))$, the only part which depends on the cosmological model. To convert our m_i data to y_i , we can adopt the value obtained from low redshift supernovae and use $\mathcal{M} = -3.40 \pm 0.05$. Defined in this way, y_i is used in other analyses [8].

After the corresponding transformations, the observables are now described by a vector of N components, y_i , and by a covariance matrix (C_y) with variance $\sigma_{y_i}^2$ and 0 otherwise.

$$C_{y,ij} = \sigma_y^2 \delta_{ij} \quad (9)$$

In the same way, the unknown parameters will be described by their *a priori* value, M_0 , and the covariance matrix (C_0). The function describing $w(z)$ should be smooth. This leads to no null covariance between neighboring points in z for $w(z)$ (the smoothness of $w(z)$ implies that if at z , the value of $w(z)$ has a deviation $w(z) - w_0(z)$ of a given sign and magnitude, we want, at a neighboring point z' , the deviation $w(z) - w_0(z)$ to have a similar sign and magnitude).

Thus, the covariance matrix C_0 has the form:

$$C_0 = \begin{pmatrix} \sigma_{\Omega_M}^2 & 0 \\ 0 & C_{w(z),w(z')} \end{pmatrix} \quad (10)$$

where several choices for non-null covariances between z and z' $C_{w(z),w(z')}$ are possible.

To stabilize the inversion (and for the smoothness constraint), we would restrict how strongly is the function allowed to fluctuate between z and z' . This would be

given by the dispersion of the function σ_w at z . We use a Gaussian choice for $C_{w(z),w(z')}$ described as:

$$C_{w(z),w(z')} = \sigma_w^2 \exp\left(-\frac{(z-z')^2}{2\Delta_z^2}\right), \quad (11)$$

which means that the variance at z equals σ_w^2 and that the correlation length between errors is Δ_z . Another possible choice is an exponential of the type:

$$C_{w(z),w(z')} = \sigma_w^2 \exp\left(-\frac{|z-z'|}{\Delta_z}\right), \quad (12)$$

while no difference in the results is found by those different choices of $C_{w(z),w(z')}$.

The best estimator \tilde{M} for M is the most probable value of M , knowing the set of data D . The approach incorporates constraints from priors through the Bayes theorem, i.e, the *a posteriori* probability density $f_{post}(M/D)$ for the vector M containing the unknown model parameters given the observed data D , is linked to the likelihood function L and the prior density function for the parameter vector as:

$$f_{post}(M/D) \propto L(D/M) \cdot f_{prior}(M) \quad (13)$$

The theoretical model described by the operator y^{th} , which connects the model parameters M with the predicted data $D_{predicted} = y^{th}(M)$ is to agree as closely as possible with the observed data y . Assuming that both the prior probability and the errors in the data are distributed as Gaussian functions, the posterior distributions becomes:

$$f_{post}(M/y) \propto \exp\left[-\frac{1}{2}(y - y^{th}(M))^* C_y^{-1} (y - y^{th}(M)) - \frac{1}{2}(M - M_0)^* C_0^{-1} (M - M_0)\right] \quad (14)$$

where $*$ stands for the adjoint operator. The best estimator for M , \tilde{M} , is the most probable value of M , given the set of data y . The condition is reached by minimizing the quantity [21]:

$$S \equiv \frac{1}{2}(y - y^{th}(M))^* C_y^{-1} (y - y^{th}(M)) + \frac{1}{2}(M - M_0)^* C_0^{-1} (M - M_0), \quad (15)$$

which is equivalent to maximize the Gaussian density of probability when data and parameters are treated in the same way. Here both data and parameters, whether directly measurable and described by their measured value and their uncertainty, or not directly measurable, described by their *a priori* information, enter in a similar

way in S . As said, the priors will be wide enough to encompass all the range of possible solutions for $w(z)$ and the uncertainty in the matter density. Generally speaking, too strict priors compared to the real *a priori* knowledge lead to biased results. However, too wide priors make the convergence of the algorithm more difficult.

As shown in Eq. 3 or equivalently Eq. 7, the inverse problem is nonlinear in the parameters, thus the solution is reached iteratively. The minimization of S proceeds using a Newton method, which allows a fast convergence of the algorithm. The explicit form of this solution for the density of matter and the equation of state is:

$$\Omega_{M[k+1]} = \Omega_{M0} + \sigma_{\Omega_M}^2 \sum_{i=1}^N W_{i[k]} \frac{\partial y_i^{th}}{\partial \Omega_M} \quad (16)$$

$$w_{[k+1]}(z) = w_o(z) + \sum_{i=1}^N W_{i[k]} \int_0^{z_i} C_w(z, z') g_w(z, z') dz' \quad (17)$$

where $W_{[k]} \equiv S_{[k]}^{-1} V_{[k]}$,

$$\begin{aligned} V_i &= y_i^{eff} + G(M - M_0) - y^{th}(M) = \\ &= y_i^{eff} + \frac{\partial y_i^{th}}{\partial \Omega_M} (\Omega_M - \Omega_{M0}) + \frac{\partial y_i^{th}}{\partial w(z)} (w - w_o) \\ &\quad - y^{th}(z, \Omega_M, w(z)) \end{aligned} \quad (18)$$

$$\begin{aligned} S_{i,j} &= C_y + G C_o G^* = \\ &= \delta_{i,j} \sigma_i \sigma_j + \frac{\partial y_i^{th}}{\partial \Omega_M} C_{\Omega_M} \frac{\partial y_j^{th}}{\partial \Omega_M} + \\ &\quad \frac{\partial y_i^{th}}{\partial w(z)} \cdot C_w \cdot \frac{\partial y_j^{th}}{\partial w(z)} \end{aligned} \quad (19)$$

and where dots in Eq. 19 represent a scalar product,

$$C_w \cdot \frac{\partial y_j^{th}}{\partial w(z)} = \int_0^z dz' C_w(z, z') g_w(z, z'), \quad (20)$$

g_w being the kernel of the derivative functional and G the matrix of partial derivatives:

$$G = \begin{pmatrix} \frac{\partial y_1^{th}}{\partial \Omega_M} & \frac{\partial y_1^{th}}{\partial w(z)} \\ \frac{\partial y_2^{th}}{\partial \Omega_M} & \frac{\partial y_2^{th}}{\partial w(z)} \\ \vdots & \vdots \\ \frac{\partial y_N^{th}}{\partial \Omega_M} & \frac{\partial y_N^{th}}{\partial w(z)} \end{pmatrix} \quad (21)$$

with

$$\begin{aligned} \frac{\partial y^{th}}{\partial \Omega_M} &= -\frac{1}{2} \int_0^{z_i} \frac{(1+z')^3 dz'}{H^3(z')} \\ &\equiv \int_0^z g_{\Omega_M}(z, z') dz', \end{aligned} \quad (22)$$

$$\begin{aligned} \frac{\partial y^{th}}{\partial w(z)} &= -\frac{1}{2} \int_0^{z_i} \frac{3\Omega_X(z') \ln(1+z') dz'}{H^3(z')} \\ &\equiv \int_0^z g_w(z, z') dz'. \end{aligned} \quad (23)$$

To test the quality of the inversion we use the *a posteriori* covariance matrix. Its value is only exact in the linear case. It is however a good approximation here, since the luminosity distance is quite linear on the equation of state $w(z)$ at low redshift.

$$C_{\tilde{M}} = C_0 - C_0 G^* S^{-1} G C_0 = (I - C_0 G^* S^{-1} G) C_0 \quad (24)$$

In a explicit form, the standard deviations from this covariance read

$$\begin{aligned} \tilde{\sigma}_{\Omega_M} &= \sqrt{C_{\tilde{\Omega}_M}} = \\ &= \sigma_{\Omega_M} \sqrt{1 - \sum_{i,j} \frac{\partial y^i}{\partial \Omega_M} (S^{-1})^{ij} \frac{\partial y^j}{\partial \Omega_M} \sigma_{\Omega_M}^2} \end{aligned} \quad (25)$$

$$\begin{aligned} \tilde{\sigma}_{w(z)}(z) &= \sqrt{C_{\tilde{w}(z)}(z)} = \\ &= \sqrt{\sigma_{w(z)}^2 - \sum_{i,j} C_w \cdot \frac{\partial y^i}{\partial w(z)} (S^{-1})^{ij} \frac{\partial y^j}{\partial w(z)} \cdot C_w} \end{aligned} \quad (26)$$

where the symbols with tilde are the *a posteriori* values, whereas the symbols without represent the *a priori* ones.

There are other parameters which help to interpret the results. From the form of Eq. 24 we see that the operator $C_0 G^* S^{-1} G$ is related to the obtained resolution. This is usually called the *resolving kernel* $K(z, z')$. The more this term resembles the δ -function the smaller the *a posteriori* covariance function is. In fact, in the linear case, the resolving kernel represents how much the results of the inversion differ from the true model. It can also be expressed in terms of only the *a priori* and the *a posteriori* covariance matrices:

$$K = I - C_{\tilde{M}} C_0^{-1} \quad (27)$$

This expression will be evaluated numerically to quantify the resolution and reliability of the results. Another term of interest is the *mean index*, which is derived from the resolving kernel:

$$I(z) = \int_0^z K(z, z') dz'. \quad (28)$$

This integrated factor tells us how much information is contained in the data. The nearest $I(z)$ to 1, the most restrictive are the data to the model. For very low values, data do not improve our prior knowledge on the parameters.

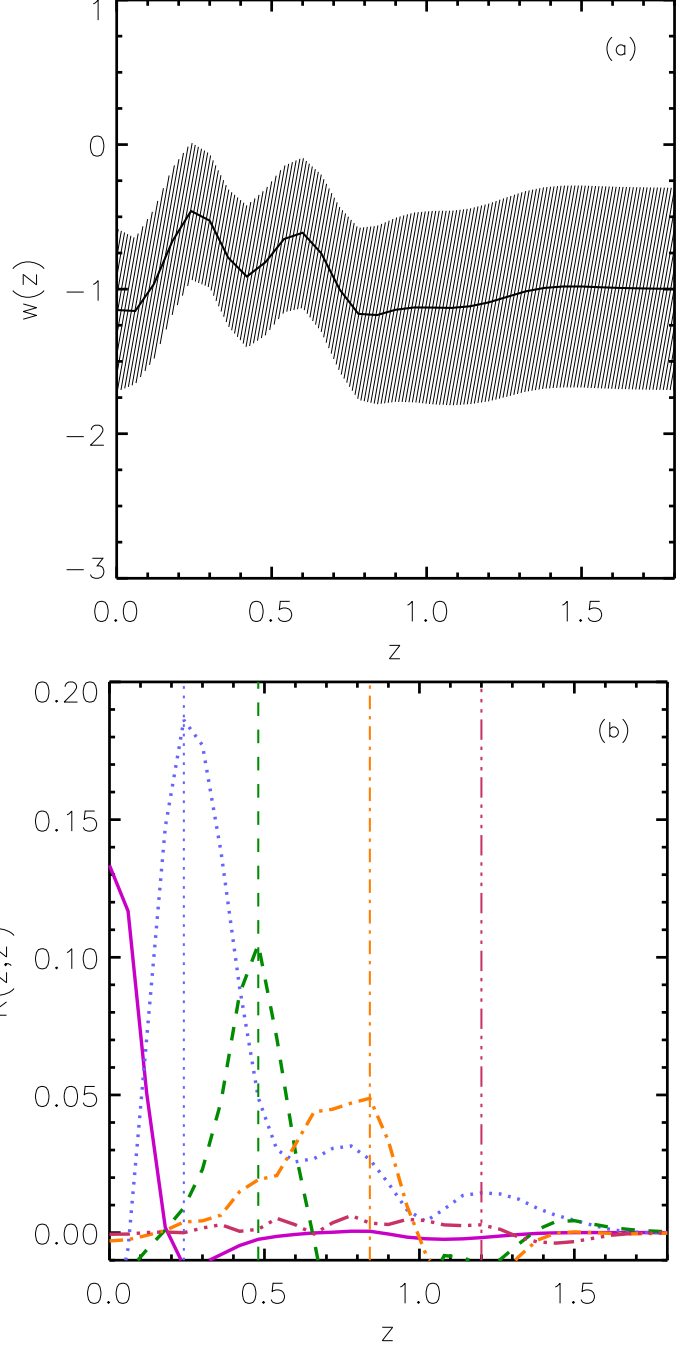


FIG. 1: Reconstruction of $w(z)$ with 156 SNe from the gold set of [20]. These results are obtained using Gaussian *a priori* covariances with amplitude $\sigma_w = 0.7$ and $\Delta_z = 0.08$. Above, it is plotted the evolution of the index of the equation of state (solid line) and the 1σ confidence interval (dashed shadow). Below, the different resolving kernels at $z = 0, 0.24, 0.48, 0.84, 1.20$ are shown. The best $K(z, z')$ is at redshift $z=0.24$. The resolving kernels at high z show that there is no information to conclude on the evolution of the equation of state at $z > 0.6$.

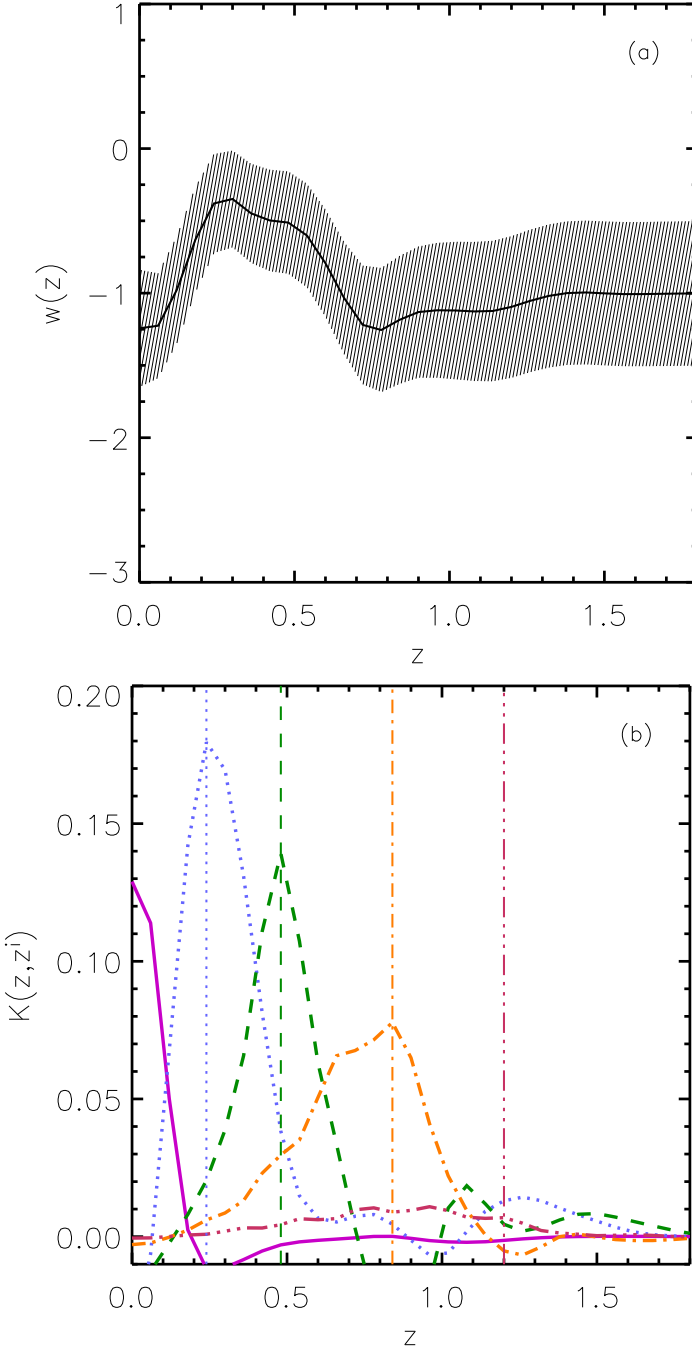


FIG. 2: It is shown $w(z)$ and $K(z, z')$ (as in Figure 1) but with the 156 SNe from the gold set of [20] and 20 RG from [8]. We have also used Gaussian covariances but now with amplitude $\sigma_w = 0.5$.

A. Particular case: only discrete parameters

In the previous section we have obtained the results for a set of a continuous function and a discrete parameter, but we can also consider the case of various discrete parameters. It was pointed out that a successful

parametrization when modeling a large variety of dark energy models is obtained by considering $w(z)$ expanded around the scale factor a [7]. The earlier parametrization to first order in z given by $w(z) = w_0 + w'z$ proved unphysical for the CMB data and a poor approach to SN data at $z \sim 1$ [16]. For the case of moderate evolution in the equation of state, the most simple (two-parameter) description of $w(z)$ so far proposed is [7]:

$$w(z) = w_0 + w_a(1 - a) \quad (29)$$

where the scale factor $a = (1 + z)^{-1}$ and $w(z)$ turns out:

$$w(z) = w_0 + w_a \frac{z}{1 + z}. \quad (30)$$

We use now this particular form for the function $w(z)$ commonly used to study the behaviour of dark energy to solve iteratively for w_0 and w_a :

$$w_{0[k+1]} = w_0^0 + \sigma_{w_0}^2 \sum_{i=1}^N W_{i[k]} \frac{\partial y_i^{th}}{\partial w_0} \quad (31)$$

$$w_{a[k+1]} = w_a^0 + \sigma_{w_a}^2 \sum_{i=1}^N W_{i[k]} \frac{\partial y_i^{th}}{\partial w_a} \quad (32)$$

where

$$\frac{\partial y^{th}}{\partial w_0} = -\frac{1}{2} \int_0^z \frac{3\Omega_X(z') \ln(1 + z') dz'}{H^3(z')}, \quad (33)$$

$$\frac{\partial y^{th}}{\partial w_a} = -\frac{1}{2} \int_0^z \frac{3\Omega_X(z')[\ln(1 + z') - \frac{z'}{1+z'}] dz'}{H^3(z')}. \quad (34)$$

The *a posteriori* variance is for these parameters:

$$\tilde{\sigma}_{w_0} = \sqrt{C_{\tilde{w}_0}} = \sigma_{w_0} \sqrt{1 - \sum_{i,j} \frac{\partial y^i}{\partial w_0} (S^{-1})^{ij} \frac{\partial y^j}{\partial w_0} \sigma_{w_0}^2} \quad (35)$$

$$\tilde{\sigma}_{w_a} = \sqrt{C_{\tilde{w}_a}} = \sigma_{w_a} \sqrt{1 - \sum_{i,j} \frac{\partial y^i}{\partial w_a} (S^{-1})^{ij} \frac{\partial y^j}{\partial w_a} \sigma_{w_a}^2} \quad (36)$$

The equations for Ω_M are those of section II (Eqs. 16, 22 and 26).

III. PRESENT AND FUTURE SAMPLES

Different data sets can be used to test the method and to extract results on $w(z)$. The first set is the 1999

data from the SCP (Supernova Cosmology Project)[1]. The set includes 16 low-redshift supernovae from the Calán/Tololo survey and 38 high-redshift supernovae used in the main fit of [1]. The second one corresponds to the gold set buildt up with 7 SNeIa at $z > 1$ by GOODS and a combination of different previous samples revised to follow the same calibrations [20]. With this second set it has been doubled the maximum redshift and triplicated the number of data as compared with the first one.

However, those samples are still small, and therefore, we also use a synthetic sample resembling the data set to be acquired by the Supernova Acceleration Probe (SNAP) [22]. To generate this sample we assume a Gaussian distribution of 2000 SNeIa data between $z=0.1$ and $z=1.7$ with maximum at $z=0.9$ and width $\sigma_z = 0.6$. For every supernova we calculate its magnitude given a fiducial dark energy model. Our first model corresponds to the cosmological constant in a universe with density parameters $\Omega_M = 0.3$ and $\Omega_\Lambda = 0.7$ (this model has $w_0 = -1$ and $w_a = 0$). We generate another synthetic sample based on a dark energy model inspired in supergravity theories (the SUGRA model analysed in [24]) with $\Omega_M = 0.3$, $w_0 = -0.8$ and $w_a = 0.6$. Gaussian errors are added to the supernova data, taking into account the intrinsic dispersion of supernovae after the corresponding calibrations ($\sigma_{intr} = 0.15$). The set of SNe is divided in bins of redshift 0.02. The magnitude corresponding to each of the 85 bins has an additional uncertainty $\sigma_{sys} = 0.02 z/z_{max}$ representing the systematics at each redshift [25]:

$$\sigma_{bin} = \sqrt{\frac{\sum \sigma_{intr}^2}{N} + \sigma_{sys}^2}. \quad (37)$$

To this distribution we also add 300 nearby SNe, as those expected from The Nearby Supernova Factory [23]. The sample amounts to 2300 SNe, i.e. 15 times more data than currently available.

One of the problems of the samples of SNeIa being gathered, is the low numbers found at $z > 1$, which reflects in the reconstruction of the equation of state. Although SNeIa are the best known calibrated candles at high redshift, the possibility of adding other luminous sources that could be reliable distance indicators to study dark energy has been advanced. Among these, the *Fanaroff-Riley type IIb radio galaxies* (FR IIb) are a group of galaxies quite homogeneous along redshift [26]. Their angular size measured from the outer edges of their lobes can be used to determine angular distances up to high z . Their possible evolution along z and selection effects have been studied [26]. We use the 20 dimensionless coordinate distances to the FR IIb radio galaxies available [8]. These data extend to $z = 1.8$, thus complements the gold set of SNeIa [20] at high redshift.

We also consider a third type of sources, compact radio sources (CRS). Extended objects of this kind have not yet been fully tested for evolutionary effects. However, a sample of 330 sources is available and they provide

distances to high z [27]. Here we use the subset with spectral index $-0.38 \leq \alpha \leq 0.18$ and total radio luminosity $Lb^2 \geq 10^{26} W/Hz$. In this way the possible dependences in angular size-spectral index and linear size-luminosity should be minimized [27]. As done in this last reference and some other subsequent analysis [28, 29], the 145 data have been binned in 12 intervals with 12 or 13 sources each, from $z = 0.52$ to $z = 3.6$ (note that this redshift is more than twice higher than that of the farthest known SN). In order to fit exclusively the parameters appearing in the equation of state a value of the characteristic length must be adopted. We use that obtained in the best fit of [28] and [29], $l = 22.64h^{-1}pc$.

Other kinds of objects such as core-collapse SNe [30] or gamma ray bursts [31] have been proposed as cosmic distance indicators observable up to very high z . Those methods have to succeed in tests of accuracy similar to those that have been successfully passed by Type Ia supernovae for the study of dark energy. Future research will address their validity. For the time being we use the data just introduced in the previous paragraphs.

IV. DETERMINATION OF $w(z)$

We present the function $w(z)$ reconstructed using the inverse approach applied to the data described above. Explicitly, one determines the value of Ω_M and w at a given redshift with the equations of section II (Eqs. 16, 17, 26 and 27).

We first need to choose an *a priori* model for these parameters. For $w(z)$ we use a covariance of the form of Eq. 11 with a moderate variance $\sigma_{\Omega_w} = 0.5 - 1.0$ and a correlation length of $\Delta_z = 0.05 - 0.10$ (see below). Larger covariances and/or larger correlation lengths cause the nonconvergence of the algorithm. We have also tried other functional forms for the covariance, such as that in Eq. 12, but no significant change or improvement has been found.

The continuous inverse approach provides the value of w at each redshift iteratively. We stop the iterative process when the difference between iterations $|w_k - w_{k-1}| < \epsilon$. The number of iterations will be typically less than 10 for ϵ of a few percent. The number of redshifts is nevertheless limited by the resolution allowed by the data. Here we will use different data sets to compare results.

The maximum resolution obtainable is dictated by the data. Demanding a finer resolution than possible can alter the results. In fact, in our case, the trends of the function $w(z)$ remain the same going to higher resolution, but both the resolving kernel and the mean index decrease. Just to give an example, after evaluating $w(z)$ intervals of $\delta z = 0.2$ in redshift (i.e ten bins) ranging from $z = 0$ to $z = 1.8$, we obtained $I(z) \sim 0.8$ in the region with richest data. The same analysis but with intervals of $\delta z = 0.06$, in the same range, diminishes the mean index up to $I(z) \sim 0.1$. In both cases the form of $w(z)$ is the same, the resolution being different. Hereafter we

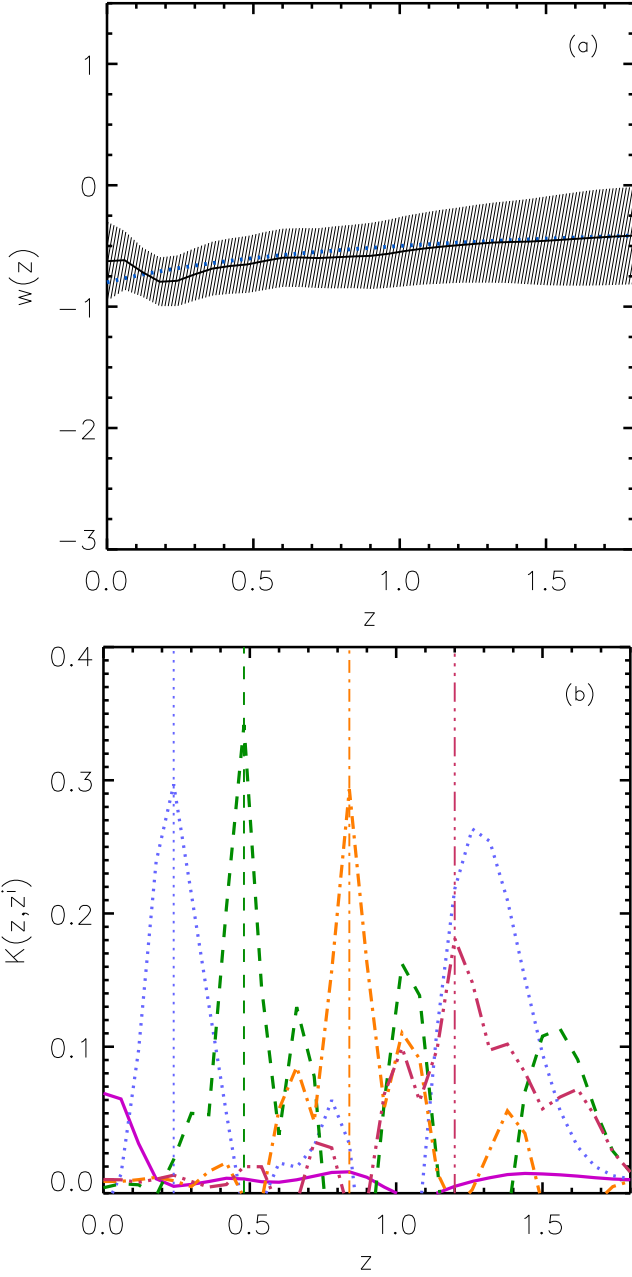


FIG. 3: Results with 2000 SNe from SNAP plus 300 SNe from SNF. All the parameters are fixed in the same way as in Figure 1 except the amplitude of the gaussian covariance, $\sigma_w = 0.4$, due to the necessity to impose a tighter prior. It is also overplotted the equation of state (short dashed line) of the fiducial dark energy model $w(z) = -0.8 + 0.6z/(1+z)$.

show the figures with finer resolution to allow a comparison with future datasets, though the corresponding mean indexes will be lower than for a coarse resolution. The choice of the correlation length Δ_z will be made accordingly, as we can not expect the two parameters to be very different and $\delta z \leq \Delta_z$.

Figure 1 shows the specific results with the 156 SNe

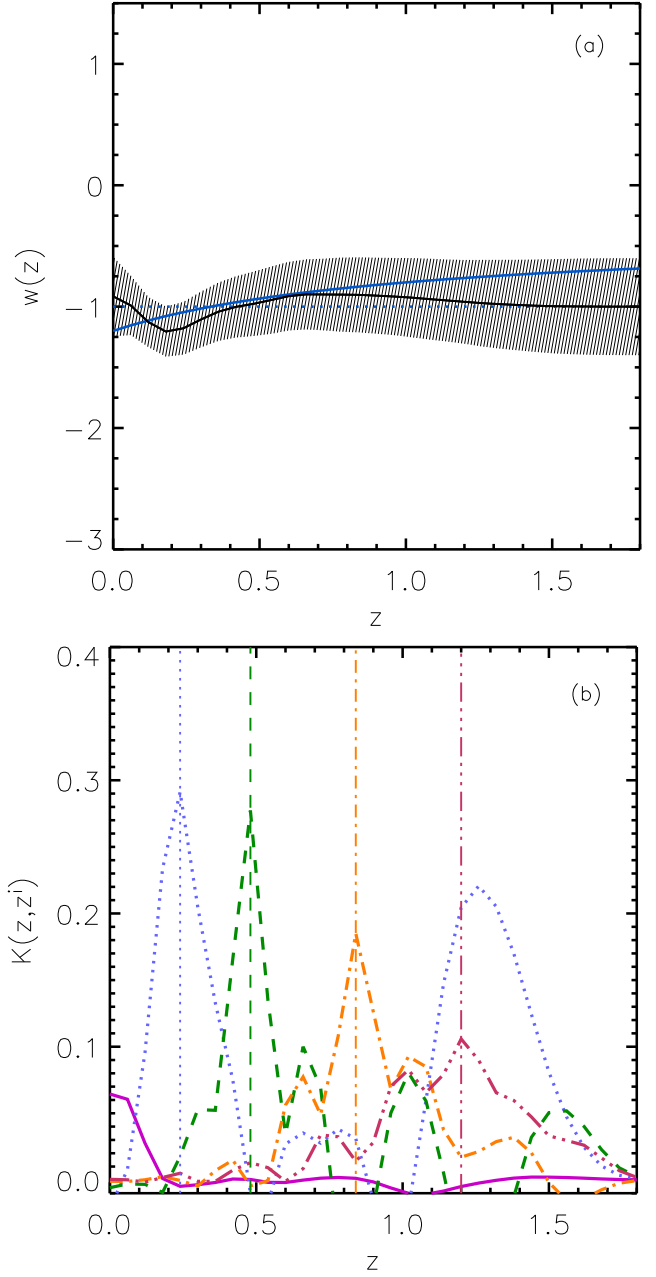


FIG. 4: The same as Figure 3, but now the fiducial model ($w(z) = -1.2 + 0.8z/(1+z)$) and the a priori one ($w(z) = -1$) are degenerate in the coordinate distance. It is then recovered the degenerate model closer to the a priori one.

from the gold set of [20]. The black solid line indicates the evolution of the equation of state, whereas the shaded region represents the 1σ interval. Although results are compatible with a cosmological constant already at the 1σ level, the ascent of $w(z)$ towards 0 at intermediate redshift is a strong feature of the reconstruction. The low resolution figure shows the same trend with high confidence (mean index near one at intermediate redshift, therefore very reliable). The two peaks are however only

seen in high resolution. The resolving kernels (low panel of the Figure 1) indicate that the function is generally not well resolved at individual redshifts, well beyond the redshift range $z \sim 0.2 - 0.3$. At high redshift, $z = 1.2$ for example, we observe a very wide and extremely flat $K(z, 1.2)$, meaning that this redshift is not resolved at all by the data. The reliability of the inversion peaks at $z \sim 0.2$ where the information is maximum.

Similar results are found when we use the set combining data from SNeIa and FR IIb radiogalaxies. The set increases only in 20 objects, but almost all of them are located at high redshift. This translates into a slightly better resolving kernels up to $z \sim 0.6$ as it can be seen in Figure 2. The equation of state is still showing the peak approaching to zero at intermediate redshifts, though that increase is not established at high confidence. Moreover, from the data gathered up to now there is no basis to infer that the positive trend from $w_0 < -1$ to an increase up to 0 at $z \sim 0.2 - 0.5$ tentatively seen continues beyond $z > 0.6$. There is no information in the data to back up such evolution beyond $z > 0.6$. In our approach, at high redshift, where there are no data, the method recovers the prior. With this larger set of data, the cosmological constant is at all z within the 2σ contour. We find similar results as in [8, 12].

We can test the method's capability to recover the equation of state using the synthetic data of SNAP simulated samples. In Figure 3 we have plotted (short dashed line) the equation of state of the fiducial dark energy model used to simulate the data: the SUGRA model in [24] with $w(z) = -0.8 + 0.6z/(1+z)$. The reconstruction has been overplotted together with 1σ uncertainties, and it can be seen that we obtain a quite good reconstruction at intermediate and high redshift, but it gets worse at low redshift. This is also seen by looking at the resolving kernel: as it happens with the previous sets of data the redshift $z = 0$ is worse determined than higher z . Another characteristic that one can deduce from the resolving kernel is the degeneracy of $w(z)$. Since *multiple peaks appear in the resolving kernel we have indications of a high degree of degeneracy of the function at those redshifts*. The dependence between the equation of state and the luminosity distance ($w(z)$) is hidden within a double integral in redshift, and thus, its variation with redshift is smoothed) eludes the uniqueness of the result. With priors away from the imposed model equation of state, we recover other solutions that are degenerate in the distance indicator. In Figure 4, our synthetic sample corresponds to an equation of state $w(z) = -1.2 + 0.8z/(z+1)$. Starting with the prior $w(z)^0 = -1.0 \pm 0.5$, we recover a degenerate solution different from the fiducial one. The fiducial model is contained in the 1σ contour of the reconstructed $w(z)$. Mapping the space of $w(z)$ one can retrieve all degenerate solutions compatible with SNAP observations through this approach. Having specific information of the value of $w(z)$ at a given z provided by other methods, more promising results for the retrieval of the continuous function $w(z)$ could be obtained. This

should be explored elsewhere.

Now, the data sets previously used in retrieving the functional $w(z)$ will be used in the determination of the discrete parameters of the value of $w(z)$ today, w_0 and its first derivative w_a .

V. INFORMATION ON w_0 AND w_a IN VARIOUS SAMPLES

We consider the three discrete unknown parameters Ω_M , w_0 and w_a , and minimize expression 15. Therefore we use Eqs. 16, 31 and 32 and make all the numerical calculations as in the previous section. We apply uninformative priors, i.e. large covariances. The convergence of the algorithm is easy for discrete parameters.

A. Results with SNe Ia

The results for Ω_M , w_0 and w_a for different *a priori* models and for the SNe sets of data mentioned in section III are shown in Table I. The first one, quoted as *P99*, corresponds to the data used in the main fit of [1]. The second one, *R04*, represents the gold set of [20]. *SNAPcc* is the SNAP simulation for the CC model and *SNAPsu* corresponds to the SUGRA one.

Here it is illustrative to look at the mean index obtained in the determination of w_0 and w_a , as it gives us an indication of the information contained in each sample of data, and how much improvement is obtained when adding more SNe Ia or other distance indicators covering wider z ranges. As in section II the mean index is obtained from the *a priori* and the *a posteriori* covariance matrices of the parameters. It shows whether the result is reliable ($I \sim 1$), and whether is highly dependent on the *a priori* model ($I << 1$).

The results indicate the difficulty to determine the variation of the equation of state, w_a with SNeIa only. The current data do not diminish the *a priori* uncertainty appreciably, and even the SNAP sample which is able to improve the *a priori* knowledge keeps large errors in w_a . The best prospects to determine w_a arise if we independently know w_0 (see, for instance, $w_0 = -1 \Rightarrow w_a = 0.0 \pm 0.2$ with SNAP). It is possible that this could be done with some other method providing a prior on w_0 . In the case of a complete ignorance of w_0 , a good degree of knowledge of Ω_M also helps to determine w_a . The error decreases by a factor 2 when we go from $\sigma_{\Omega_M} = 0.04$ to $\sigma_{\Omega_M} = 0$.

If we only aim at determining w_0 , the results are already well established. Recent data from [20] already determine it up to a 10% ($w_0 = -1.0 \pm 0.1$) when it is assumed a constant equation of state and fixed knowledge for the matter density parameter Ω_M . Allowing a variation of Ω_M ($\sigma_{\Omega_M} = 0.04$), the uncertainty increases to 15% ($w_0 = -0.98 \pm 0.16$). The synthetic data from

TABLE I: Priors and results for Ω_M , w_0 and w_a . Values in parentheses reflect the error of the parameter in the last digit. To see the reliability of the result the mean index, I , is shown. Imposing a prior $-1(0)$ for w_0 means that we force the result to be cosmological constant now. Alternatively, a prior of w_a with value $0(0)$ forces no evolution. Generally, the most interesting case is when priors are wide: $\Omega_M = 0.30(4)$, $w_0 = -1(10)$ and $w_a = 0(10)$ and there are no restrictions (results outlined in boldface).

	Ω_M	I_{Ω_M}	w_0	I_{w_0}	w_a	I_{w_a}
<i>Prior</i>	<i>0.30(0)</i>	-	<i>-1(10)</i>	-	<i>0(0)</i>	-
P99	0.30(0)	-	-1.0(2)	0.999	0(0)	-
R04	0.30(0)	-	-1.0(1)	0.999	0(0)	-
SNAPcc	0.30(0)	-	-0.99(3)	0.999	0(0)	-
SNAPsu	0.30(0)	-	-0.68(3)	0.999	0(0)	-
<i>Prior</i>	<i>0.30(4)</i>	-	<i>-1(10)</i>	-	<i>0(0)</i>	-
P99	0.30(3)	0.245	-1.0(2)	0.999	0(0)	-
R04	0.29(3)	0.540	-1.0(2)	0.999	0(0)	-
SNAPcc	0.32(3)	0.478	-1.0(1)	0.999	0(0)	-
SNAPsu	0.29(3)	0.571	-0.7(1)	0.999	0(0)	-
<i>Prior</i>	<i>0.30(4)</i>	-	<i>-1(10)</i>	-	<i>0(10)</i>	-
P99	0.30(4)	0.193	-1.5(7)	0.995	+4(5)	0.739
R04	0.31(3)	0.495	-1.3(4)	0.998	+2(2)	0.951
SNAPcc	0.31(3)	0.505	-0.9(3)	0.999	-1(1)	0.965
SNAPsu	0.30(3)	0.454	-0.7(2)	0.999	+0.3(7)	0.994
<i>Prior</i>	<i>0.30(4)</i>	-	<i>-1(0)</i>	-	<i>0(10)</i>	-
P99	0.29(3)	0.383	-1(0)	-	+0(2)	0.975
R04	0.27(2)	0.669	-1(0)	-	+0.6(8)	0.994
SNAPcc	0.33(2)	0.709	-1(0)	-	+0.0(2)	0.999
SNAPsu	0.38(2)	0.778	-1(0)	-	+0.7(5)	0.997

SNAP give less than a 5% of error in w_0 with a mean index of 0.999.

When reading in Table I the mean index for Ω_M , we have to realize that it has to be low, as we already start from a low value of the uncertainty ($\sigma_{\Omega_M} = 0.04$), and data can not improve it too much. An uncertainty of such order is expected from methods using galaxy clusters. The mean index obtained placing that prior and using SNe Ia and other distance indicators to improve the knowledge of Ω_M , just indicates that we had from the beginning a good knowledge on the parameter and the data can not improve a lot its uncertainty although

the fit is good.

Finally we compare the results obtained with this kind of inverse approach with the ones obtained in [20]. Results should be similar when the χ^2 -test is complemented with Gaussian *a priori* information, since in both cases we want the same likelihood to be maximum. In [20] a prior of $\Omega_M = 0.27 \pm 0.04$ in a flat universe with a constant $w(z) = w_0$ leads to $w_0 = -1.02 \pm 0.13$. We do the same and obtain $w_0 = -0.90 \pm 0.14$ with large confidence: $I = 0.999$. The two methods show agreement. When testing the evolution using a development of the equation of state of the form $w(z) = w_0 + w'z$, with the same priors as before, results in $w_0 = -1.31 \pm 0.22$ and $w' = 1.48 \pm 0.90$ in Riess analysis. We prefer the two-parameter expansion in terms of w_0 and w_a , as we see that the linear expansion in z incorporates poorly the information in the inversion (and produces low reliability indexes). With the inverse method, we find: $w_0 = -1.3 \pm 0.4$ and $w_a = 2 \pm 2$, which corresponds at z around 0.3 to $w' = 1.5 \pm 1.5$. We take instead of $\Omega_M = 0.27 \pm 0.04$, the slightly larger value $\Omega_M = 0.3 \pm 0.04$. When using FRIIb and SNe Ia, we have a similar result with half the error $w_a = 2 \pm 1$.

TABLE II: The same as Table I but now priors and results are for models of evolving CC with parameters $\Omega_M (= 1 - \Omega_\Lambda)$ and $(1/\rho_c^0)d\Lambda/dz|_0$.

	Ω_M	I_{Ω_M}	$\frac{1}{\rho_c} \frac{d\Lambda}{dz} _0$	$I_{d\Lambda}$
<i>Prior</i>	<i>0.30(4)</i>	-	<i>0(10)</i>	-
P99	0.30(3)	0.262	0.0(4)	0.998
R04	0.29(3)	0.555	0.0(3)	0.999
SNAPcc	0.31(3)	0.536	-0.1(2)	0.999
SNAPsu	0.30(3)	0.513	+0.7(2)	0.999
<i>Prior</i>	<i>0.30(10.0)</i>	-	<i>0(10)</i>	-
P99	0.28(7)	0.999	+0.1(7)	0.995
R04	0.29(4)	0.999	+0.1(4)	0.998
SNAPcc	0.32(4)	0.999	-0.2(3)	0.999
SNAPsu	0.30(4)	0.999	+0.7(3)	0.998

Some models of dark energy are not well parameterized using an equation of state with w_0 and w_a (or w_0 and w'). Here we investigate how this inverse approach works for the varying cosmological constant models. The background of those models is that quantum effects near the Planck scale would cause the evolution of the CC (see [32, 33]). The best way to parameterize the dark energy density along z representing all this branch of models is through:

$$\Omega_X(z) = \Omega_\Lambda^0 + \frac{1}{\rho_c^0} \frac{d\Lambda}{dz} \Big|_0 z \quad (38)$$

Thus, we have implemented the inverse approach for this branch of models and find the results for the two discrete parameters that are to first order describing this dark energy candidate. Those are $\Omega_M (= 1 - \Omega_\Lambda)$ and $(1/\rho_c^0)d\Lambda/dz|_0$. Results are shown in Table II. Although present-day data are consistent with a non-variation of the CC, a small running is allowed. These results can be compared with those from [33], where similar conclusions were reached through a χ^2 -test analysis.

The Table II also reflects the effect of the prior on the mean index. Different values within the uncertainty of Ω_M cause a large variation in its mean index, though the best determination for the parameter remains almost unchanged.

The simulation using a SUGRA fiducial model with $w_0 = -0.8$ and $w_a = +0.6$ as observed by SNAP, shows that the data set is degenerate with a Λ -varying model with $(1/\rho_c^0)d\Lambda/dz|_0 = +0.7$. A Λ -varying model such as those proposed [32] results in observables that, if interpreted through w_0 and w_a , might suggest a model with quite different physics.

Overall, degeneracies found in the solution of $w(z)$ and the existence of models apparently indicating an evolving $w(z)$ but reflecting other physics, will make necessary to analyse the set of possible theories compatible with the SNAP observations.

B. Combining SNeIa with other sources

In the previous subsection, we have only used a specific type of data to study the equation of state: SNeIa. Combining them with the other sources introduced in section III will increase considerably the number of data at very high redshift. We see that going to higher redshifts has a similar effect than increasing significantly the number of data in experiments such as SNAP.

As can be seen in Table III, using the three kinds of cosmic distance indicators reduces the uncertainty in the first derivative of the equation of state w_a by 50% in respect to the use of SNeIa. Although data from CRS extend to $z = 3.6$, we obtain similar results by only adding 20 FRIIb radiogalaxies which reach up to $z = 1.8$. This happens because the dispersion of CRS data, is much bigger than for radiogalaxies and, evidently, than for SNeIa. Therefore, having more data at higher redshift is compensated by the large dispersion.

As a difference with the gold set of [20] (results in Table I) we observe a positive evolution of the equation of state ($w_a > 0$) at almost 2σ level when more than a set of data is considered. In this case (an evolving equation of state) the value of $w_0 = -1$ lies outside the 1σ contours.

Different samples of distance indicators might favor slightly different results. As seen in Fig. 2, evolution

TABLE III: Priors, results and mean index for Ω_M , w_0 and w_a but for different kinds of sources: SNeIa gold set (SN), FRIIb radio galaxies (RG), compact radio sources (CRS) and combinations among them.

	Ω_M	I_{Ω_M}	w_0	I_{w_0}	w_a	I_{w_a}
<i>Prior</i>	<i>0.30(4)</i>	-	<i>-1(10)</i>	-	<i>0(0)</i>	-
SN	0.29(3)	0.540	-1.0(2)	0.999	0(0)	-
RG	0.30(4)	0.010	-0.8(2)	0.999	0(0)	-
CRS	0.30(4)	0.001	-0.8(3)	0.998	0(0)	-
SN+RG	0.23(2)	0.688	-0.9(1)	0.999	0(0)	-
SN+CRS	0.24(2)	0.689	-0.9(1)	0.999	0(0)	-
all	0.23(2)	0.688	-0.9(1)	0.999	0(0)	-
<i>Prior</i>	<i>0.30(4)</i>	-	<i>-1(10)</i>	-	<i>0(10)</i>	-
SN	0.31(3)	0.495	-1.3(4)	0.998	+2(2)	0.951
RG	0.30(4)	0.193	0(1)	0.988	-6(7)	0.492
CRS	0.30(4)	0.015	0(1)	0.984	-3(7)	0.518
SN+RG	0.28(2)	0.640	-1.3(3)	0.999	+2(1)	0.979
SN+CRS	0.28(2)	0.642	-1.4(3)	0.999	+2(1)	0.982
all	0.27(2)	0.647	-1.3(3)	0.999	+2(1)	0.984
<i>Prior</i>	<i>0.30(4)</i>	-	<i>-1(0)</i>	-	<i>0(10)</i>	-
SN	0.27(2)	0.669	-1(0)	-	+0.6(8)	0.994
RG	0.31(4)	0.055	-1(0)	-	+0(1)	0.981
CRS	0.30(4)	0.027	-1(0)	-	+1(2)	0.976
SN+RG	0.22(2)	0.803	-1(0)	-	+1.2(4)	0.998
SN+CRS	0.21(2)	0.808	-1(0)	-	+1.2(4)	0.998
all	0.22(2)	0.810	-1(0)	-	+1.2(4)	0.998

is only tentatively suggested at $z \sim 0.3$. Trends of evolution at high z can not be determined with the available data, as those redshifts are very poorly determined.

VI. ESTIMATING THE BEST DISTRIBUTION OF DATA

As an application of this parametric reconstruction of the equation of state we use the method to obtain the distribution of data which recovers the fiducial model with the best possible quality in the inversion.

The samples synthesized are Gaussian distributions centered at different redshifts (z_0) with different widths (σ_z). The total number of SNe is 2000 between 0 and 2.5 (samples of the size of SNAP), plus another Gaussian distribution of 300 SNe centered at $z = 0.05$ and representing data coming from [23]. In this way we have generated a total of 143 distributions which cover the

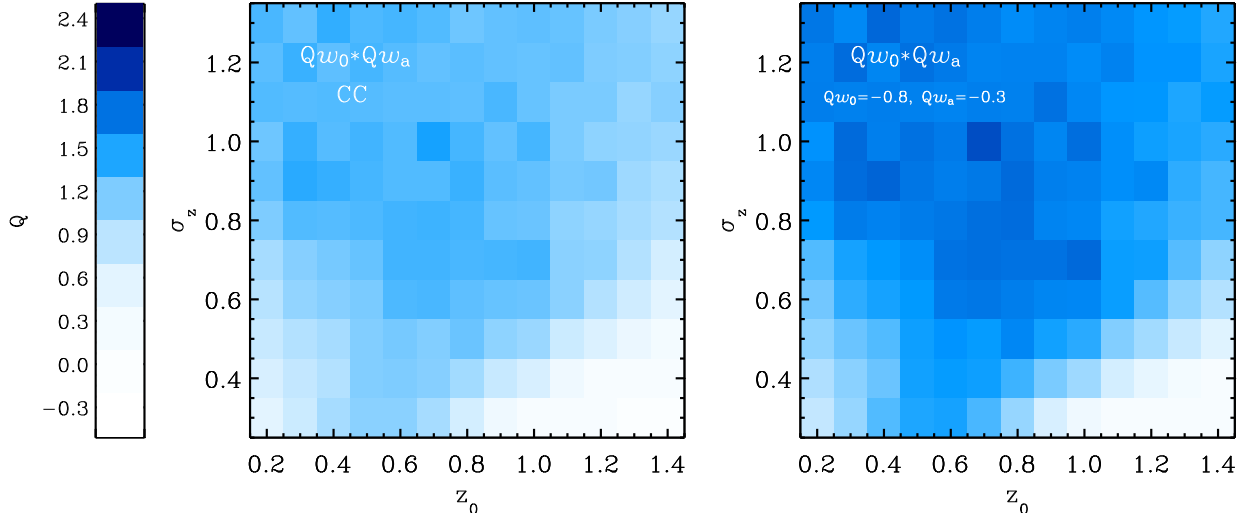


FIG. 5: Product of the quality factors Q . Different Gaussian distributions of data are indicated by the center of the distribution (z_0) and its width (σ_z). Colors represent the quality level of the inversion, in logarithmic scale, being the darkest zone the one with best inversion. From left to right we have plotted a fiducial model of CC, and a model with negative sign in the evolution: $w_0 = -0.8$ and $w_a = -0.3$.

ranges $0.2 < z_0 < 1.4$ and $0.3 < \sigma_z < 1.3$ at intervals of 0.1 in both parameters. We produce these distributions for different dark energy models: 1) CC with $\Omega_M = 0.3$, $\Omega_\Lambda = 0.7$, $w_0 = -1$ and $w_a = 0$, 2) SUGRA with $\Omega_M = 0.3$, $w_0 = -0.8$ and $w_a = 0.6$, 3) a similar model but with a negative evolution $\Omega_M = 0.3$, $w_0 = -0.8$ and $w_a = -0.3$, and finally 4) a model with an evolving CC $\Omega_M = 0.3$, $\Omega_\Lambda = 0.7$, $(1/\rho_c^0)d\Lambda/dz|_0 = 0.1$.

For each of these distributions we invert the data to obtain w_0 and w_a , assuming $\Omega_M = 0.3$.

We can find the distribution that provides the *best* quality of the inversion. This *quality* is higher the smaller the dispersion in the results (σ_{w_0} , σ_{w_a}), and the closest the result is to the seed one ($|w_0 - w_0^{seed}|$, $|w_a - w_a^{seed}|$). Thus we define a quality factor of the inversion for each parameter as $Q_{w_0} = \log(\sigma_{w_0}|w_0 - w_0^{seed}|)^{-1}$ and $Q_{w_a} = \log(\sigma_{w_a}|w_a - w_a^{seed}|)^{-1}$.

The results are shown in Figure 5. Zones with dark blue represent distributions with the highest quality of the inversion, whereas the lightest zone are those with a low quality, as shown in the color scale next to the figures.

The first panel shows the results for a fiducial model of CC inverted using these “seed” values as *a priori*. We have first calculated the individual qualities Q_{w_0} and Q_{w_a} and observed that *all the distributions determine much better w_0 than w_a* . We have already seen this fact in the SNAP results of the previous section, but it is a common characteristic in all cases. Furthermore, distributions centered only at high redshift give very poor results even for w_a . When we join together the qualities in both parameters we see more clearly that there is another poor section at low redshift with a small width. This kind of

distributions could represent those from the initial samples [1] but with larger number of data. Thus we see the need to extend the number of data at redshift $z > 1$. This has been started within the GOODS ACS Treasury Programme [34], and will continue by the SCP and other collaborations to improve the study of dark energy.

The second panel present a model different than the CC. It has common features to the dark energy models tried. Perhaps it is worth clarifying that while Figure 5 shows the results of inversions done with the same prior as the seed model, we have always used large uncertainties in the preferred value of the prior. Changing the center of the prior does not change at all the results. We observe the preference for the same region of data ($z_0 \sim 0.7$ and $\sigma_z \sim 1$) in the CC case and in other dark energy models such as those relating to SUGRA or those with a negative evolution in z (in the second panel $\Omega_M = 0.3$, $w_0 = -0.8$ and $w_a = -0.3$). We have also studied the quality for the models with a running CC (Eq. 38) where, since the evolution is more important at larger redshift, wide distributions of data at high redshift are the optimal ones. However, all the distributions give a good quality of the inversion in the running CC models.

VII. SUMMARY AND DISCUSSION

We present here the results of an Inverse Problem approach applied to determine $w(z)$ as a continuous function in a model-independent and non-parametric way. The method enables to examine $w(z)$ without imposing any constraints in the form of the function. The results allow to evaluate whether there is evidence in the evolution of $w(z)$ along z if we consider the data gathered using SNe Ia

and other cosmological distance indicators. We find that the highest degree of information on $w(z)$ from present samples is at $z \sim 0.2$. The current SNe Ia data indicate a tendency towards $w = 0$ at those intermediate redshifts. However, though this feature is consistently found in the analysis (and when using broad redshift bins, it is found at a mean index $I(z)$ close to 1), the cosmological constant is still within the 2σ level contours of the solution $w(z)$ up to high z . Moreover, it is found that there is no information on $w(z)$ at $z > 0.6$ to imply any possible evolution of $w(z)$ at those z .

Retrieving $w(z)$ will improve when using a large sample of SNeIa data and data at $z > 1$ possibly contributed by other cosmological probes. However, there will be a number of degenerate solutions compatible with the data that can make difficult to derive physical consequences. This approach allows to evaluate the reliability of the fit and the resolution obtained in $w(z)$ in redshift space. Addressing the study of the equation of state of dark energy in the simplest two-parameter form (by obtaining the present value and its first derivative, w_0 and w_a), we have seen how information has improved in the samples obtained during the last years. Adding FR IIb radio-galaxies to SNe Ia to determine the uncertainty in w_a is

reduced by 50% and $w_a = 2 \pm 1$ ($w_0 = -1.3 \pm 0.3$, in agreement with other analyses). Within these two-parameter simplified analysis, we have studied the distribution of SNe Ia data that allows a best reconstruction of $w(z)$ for a range of models representing various possible dark energy candidates. Generating alternative distributions of data we see that the best quality when inverting the observables to recover the unknown parameters of the equation of state is provided by data sets with broad distributions ($\sigma_z \sim 1$) reaching to high z and centered at $z_0 \sim 0.7$. Those results are in agreement with results from Monte Carlo simulations.

Acknowledgments

This work has been partially supported by the European Research and Training Network Grant on Type Ia Supernovae (HPRN-CT-20002-00303), and by research grants in cosmology by the Spanish DGCYT (ESP20014642-E and BES-2004-4435) and Generalitat de Catalunya (UNI/2120/2002).

[1] S. Perlmutter et al., *Astrophys. J.*, **517**, 565 (1999)
[2] A.G. Riess et al., *Astron. J.*, **116**, 1009 (1998)
[3] D.N. Spergel et al., *Astrophys. J. Suppl. Ser.*, **148**, 175 (2003)
[4] W.J. Percival et al., *Mon. Not. R. Astron. Soc.*, **327**, 1297 (2001)
[5] S.W. Allen et al., *Mon. Not. R. Astron. Soc.*, **342**, 287 (2003)
[6] B.F. Gerke and G. Efstathiou, *Mon. Not. R. Astron. Soc.*, **335**, 33 (2002)
[7] E.V. Linder, *Phys. Rev. Lett.*, **90**, 091301 (2003)
[8] R.A. Daly and S.G. Djorgovski, *Astrophys. J.*, **612**, 652 (2004) [[astro-ph/0403664](#)]
[9] M. Visser, *Class. Quant. Grav.* **21** (2004) [[gr-qc/0309109](#)]
[10] S. Nesseris and L. Perivolaropoulos, *Phys. Rev. D*, **70**, 043531 (2004)
[11] D. Huterer and G. Starkman, *Phys. Rev. Lett.*, **90**, 031301 (2003)
[12] D. Huterer and A. Cooray, [[astro-ph/0404062](#)] (2004)
[13] U. Alam, V. Sahni, T. Deep Saini & A.A. Starobinsky, *Mon. Not. R. Astron. Soc.*, **354**, 275 (2003)
[14] U. Alam, V. Sahni, A.A. Starobinsky, *JCAP*, **0406**, 008 (2004) [[astro-ph/0403687](#)]
[15] J. Jönsson, A. Goobar, R. Amanullah & L. Bergström, [[astro-ph/0404468](#)] (2004)
[16] E.V. Linder, [[astro-ph/0210217](#)] (2002)
[17] G. Backus and F. Gilbert, *Philos. Trans. R. Soc. London. Ser. A.*, **366**, 123 (1970)
[18] I. Maor, R. Brustein & P.J. Steinhardt, *Phys. Rev. Lett.*, **86**, 6 (2001)
[19] I. Maor and R. Brustein, *Phys. Rev. D*, **67**, 103508 (2003)
[20] A.G. Riess et al., *Astrophys. J.*, **607**, 665 (2004)
[21] A. Tarantola and B. Valette, *Rev. Geophys. & Space Phys.*, **20**(2), 219 (1982); A. Tarantola, 1987, *Inverse Problem Theory*, Elsevier, Amsterdam
[22] SNAP collaboration, <http://snap.lbl.gov/>
[23] The Nearby Supernova Factory collaboration, <http://snfactory.lbl.gov/>
[24] J. Weller and A. Albrecht, *Phys. Rev. Lett.*, **86**, 1939 (2001)
[25] A. G. Kim, E.V. Linder, R. Miquel and N. Mostek, *Mon. Not. Roy. Astron. Soc.* **347**, 909 (2004), [astro-ph/0304509](#)
[26] R.A. Daly and E.J. Guerra, *Astron. J.*, **124**, 1831 (2002); R.A. Daly and S.G. Djorgovski, *Astrophys. J.*, **597**, 9 (2003)
[27] L.I. Gurvits, K.I. Kellermann & S. Frey., *Astron. Astrophys.*, **342**, 378 (1999)
[28] J.A.S. Lima and J.S. Alcaniz, *Astrophys. J.*, **566**, 15 (2002)
[29] Z.H. Zhu et al., *Astron. Astrophys.*, **417**, 833 (2004)
[30] D.C. Leonard et al., *PASP*, **114**, 35L (2002)
[31] Z.G. Dai, E. W. Liang and D. Xu, *Astrophys. J.*, **612**, 101 (2004); B. E. Schaefer, *Astrophys. J.* **583**, L67 (2003)
[32] M. Reuter, C. Wetterich, *Phys. Lett. B* **188**, 38 (1987); I.L. Shapiro and J. Solà, *J. High Energy Phys.*, **202**, 006 (2002); A. Babic, B. Guberina, R. Horvat, H. Stefancic, P, *Phys. Rev. D*, **65**, 085002 (2002); A. Bonanno and M. Reuter, *Phys. Rev. D*, **65**, 043508 (2002); I.L. Shapiro, J. Sola, C. España-Bonet, P. Ruiz-Lapuente, *Phys. Lett. B*, **574**, 149 (2003); J.W. Moffat, [astro-ph/0412195](#) (2004); F. Bauer, preprint [gr-qc/0501078](#) (2005)
[33] C. España-Bonet, P. Ruiz-Lapuente, I. L.Shapiro and J. Solà, *J. Cosmol. Astropart Phys.*, **0402**, 006 (2004)
[34] GOODS project <http://www.stsci.edu/science/goods>